

# A Self-Distillation Embedded Supervised Affinity Attention Model for Few-Shot Segmentation

Qi Zhao, *Member, IEEE*, Binghao Liu, Shuchang Lyu, *Student Member, IEEE*, Xu Wang, and Lijiang Chen

**Abstract**—Few-shot semantic segmentation is a challenging task of predicting object categories in pixel-wise with only few annotated samples. However, existing approaches still face two main challenges. First, huge feature distinction between support and query images causes knowledge transferring barrier, which harms the segmentation performance. Second, few support samples cause unrepresentative of support features, hardly to guide high-quality query segmentation. To deal with the above two issues, we propose self-distillation embedded supervised affinity attention model (SD-AANet) to improve the performance of few-shot segmentation task. Specifically, the self-distillation guided prototype module (SDPM) extracts intrinsic prototype by self-distillation between support and query to capture representative features. The supervised affinity attention module (SAAM) adopts support ground truth to guide the production of high quality query attention map, which can learn affinity information to focus on whole area of query target. Extensive experiments prove that our SD-AANet significantly improves the performance comparing with existing methods. Comprehensive ablation experiments and visualization studies also show the significant effect of SDPM and SAAM for few-shot segmentation task. On benchmark datasets, PASCAL-5<sup>i</sup> and COCO-20<sup>i</sup>, our proposed SD-AANet both achieve state-of-the-art results. Our code is available on <https://github.com/cv516Buaa/SD-AANet>.

**Index Terms**—Few-shot Segmentation, Few-shot Learning, Self-distillation, Attention Mechanism.

## I. INTRODUCTION

SEMANtic segmentation, as a significant computer vision task, aims to assign a class label to each pixel in the image. Fully convolutional networks (FCNs) [1] have been the pioneer to handle this task in an end-to-end manner, then various of deep neural network models [2]–[8] have made great improvements recently. However, massive pixel-level annotated data required in semantic segmentation leads to expensive annotation cost. In addition, these methods have a dramatically performance decline when meeting unseen classes.

To address above-mentioned issues, few-shot segmentation [9] is proposed using few annotated data to segment unseen classes. Different from fully supervised semantic segmentation, few-shot segmentation splits the whole data into support set and query set. The support set in this task provides meaningful and critical features of certain class to guide algorithm extracting target of same class in query set.

Current few-shot segmentation methods are mainly based on metric learning, containing two main technical routes:

Q. Zhao, B. Liu, S. Lyu, X. Wang and L. Chen are with the Department of Electronic and Information Engineering, Beihang University, 37 Xueyuan Road, Haidian District, Beijing, P.R. China, 100191. (e-mail: zhaohq@buaa.edu.cn, liubinghao@buaa.edu.cn, lyushuchang@buaa.edu.cn, sy2002406@buaa.edu.cn, chenlijiang@buaa.edu.cn).

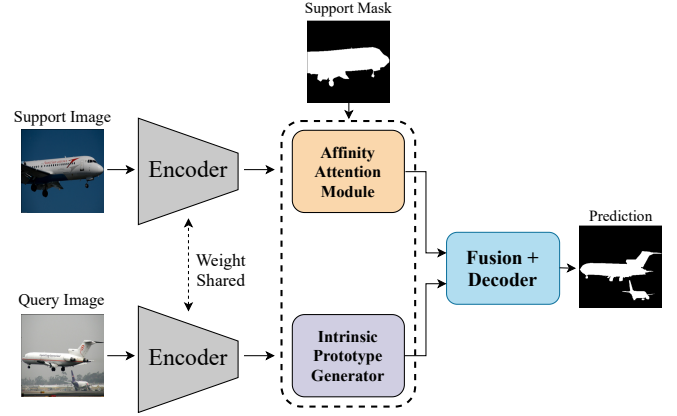


Fig. 1. Overview of SD-AANet. SD-AANet contains four modules which are Encoder, SDPM, SAAM and Decoder. Encoder is a CNN backbone to extract features of inputs. SDPM obtains intrinsic prototype by introducing self-distillation approach. SAAM learns a query attention by support predict supervision. Then the fusion of intrinsic prototype, query feature and query attention are input to decoder to get final prediction.

affinity learning [10]–[12] and prototypical learning [13]–[15]. Affinity learning acquires feature of support object with the help of support label. Then each pixel-wise feature belonging to the support image is matched to pixel-wise feature at the same position of query image through various correlation measure operations, guiding query segmentation.

Prototypical learning methods usually uses one or few prototypes to represent support object feature and guide segmentation of query target. These methods adopt masked global average pooling (masked GAP) [13] to obtain support prototypes. Generally, the support prototype is combined with query feature through correlation metrics to realize high-quality segmentation.

However, existing methods still have two major weaknesses. First, the appearance of objects in images may have different quantities, perspectives, illumination intensities and etc. Previous methods can not apply abundant and representative support information to guide query target segmentation. Second, few support samples can not provide sufficient representative information. Some typical failure cases of existing methods can be seen in Fig. 2.

To deal with issue caused by image distinctions, we propose a novel module named self-distillation guided prototype generating module (SDPM), which adopts self-distillation approach to close the gap between support and query features. SDPM takes support label, support feature and query feature as inputs, producing a reweighting query feature and a support prototype with intrinsic feature.

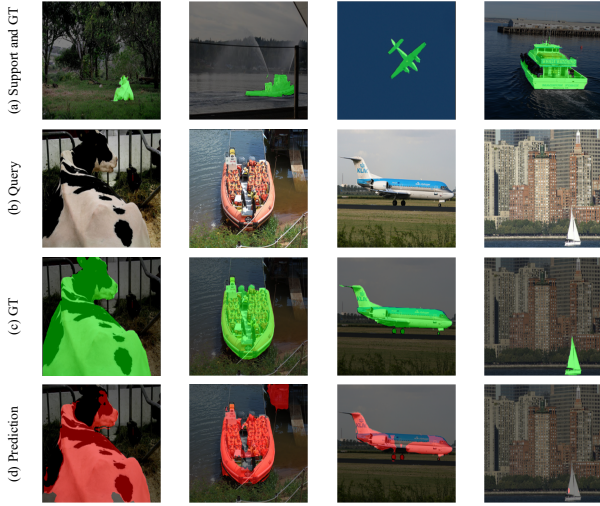


Fig. 2. Some failure cases of current methods. From top to bottom: (a) support image and its ground truth, (b) query image, (c) ground truth of query image, (d) prediction of current methods.

In few-shot segmentation task, one or few support samples can not provide representative information to segment the query target. So we design the supervised affinity attention module (SAAM), a CNN-based end-to-end module which can simply embed in deep CNN models and introduce negligible computation cost. SAAM has the same inputs as SDPM, is used to generate a prior prediction of support image and an affinity attention map of query image.

Based on the two modules mentioned above, we propose the self-distillation embedded affinity attention model (SD-AANet), combining SDPM and SAAM, to produce intrinsic prototype and affinity attention map efficiently. Overview of the SD-AANet is illustrated in Fig. 1. Extensive experiments show that our SD-AANet achieves state-of-the-art performance on PASCAL-5<sup>i</sup> and COCO-20<sup>i</sup> datasets.

Our contributions are summarized as follows:

- We propose the SDPM to efficiently reduce the influence of images' distinction, which contains a intrinsic prototype generated by introducing a self-distillation approach.
- By combining a support cross-entropy supervision and trainable affinity feature extractor, our SAAM helps capturing a high quality attention map to teach decoder where to focus.
- SD-AANet achieves new state-of-the-art results on both PASCAL-5<sup>i</sup> [9] (mIoU for 1-shot: 61.9%, 5-shot: 64.4%) and COCO-20<sup>i</sup> [16], [17] datasets (mIoU for 1-shot: 39.6%, 5-shot: 47.4%) for this task.

## II. RELATED WORK

### A. Semantic Segmentation

Semantic Segmentation aims to predict a semantic category for each pixel in image. Convolutional Neural Network (CNN) based methods have made great progress in semantic segmentation field. Fully convolutional networks (FCN) [1] replaces fully connected layers with convolutional layers, achieving semantic segmentation in an end-to-end manner. SegNet [2] and

UNet [3] employ symmetric “Encode-Decoder” architectures to map the original image to the same-size predictions. PSPNet [6] integrates pyramid pooling module into several baseline architectures like ResNet [18], [19]) to obtain contextual information from different scales by using different kernel-sized pooling layers. Chen et al. [20], [21] employ dilated convolution to expand the receptive field. In addition, some works focus on attention mechanism. PSANet [22] proposes a point-wise spatial attention to explore better connection information between pixels. DANet [23] adopts position attention module and channel attention module to learn position and channel inter-dependencies. CCNet [24] adopts a criss-cross attention module to capture contextual information from full-image dependencies. However, well-performed semantic segmentation networks need a large amount of annotations as training samples that are expensive to obtain.

### B. Few-shot learning

Few-shot Learning seeks to recognize new objects with only few annotated samples. In this field, as an interpretable approach, metric learning [25], [26] is widely used. Koch et al. [25] propose a siamese architecture which shows great performance on k-shot image classification tasks. This architecture can also be extended to deal with k-shot semantic segmentation. Meta learning [27] enables machine to quickly acquire useful prior information from limited labeled samples. Meta-learning LSTM [28] and Model-Agnostic [29] methods apply recurrent neural network (RNN) to represent and store the prior information to handle the few-shot problem. To own the advantage of both two methods, ProtoMAML [30] combined the complementary strengths of metric-learning and gradient-based meta-learning methods.

### C. Few-shot Segmentation

Few-shot Semantic Segmentation aims at performing dense pixel-wise classification for unseen classes. Caelles et al. [31] propose an effective approach to achieve one-shot video segmentation by fine-tuning a pretrained segmentation network on few labeled images of unseen categories. Shaban et al. [9] are the pioneers to officially define the few-shot semantic segmentation problem. They propose a two-branch architecture (OSLSM) to produce a binary mask for the new semantic class with dot-similarity manner. Rakelly et al. [32], Dong et al. [33] and Hu et al. [34] extend two-branch based approach and achieve better performance than OSLSM. SG-One [13] propose an architecture consist of a guidance branch and a segmentation branch which is now the benchmark architecture in one-shot segmentation task.

In recent years, many works are based on SG-One. PANet [35] learns class-specific prototype representations from support image within an embedding space and then performs segmentation over the query image through matching each pixel to the learned prototypes. CANet [14] continues to follow the similarity guidance strategy and add iterative optimization module to refine the final prediction. PFENet [36] proposes a training-free prior generation process to produce prior segmentation attention for the model, and a feature enrichment module

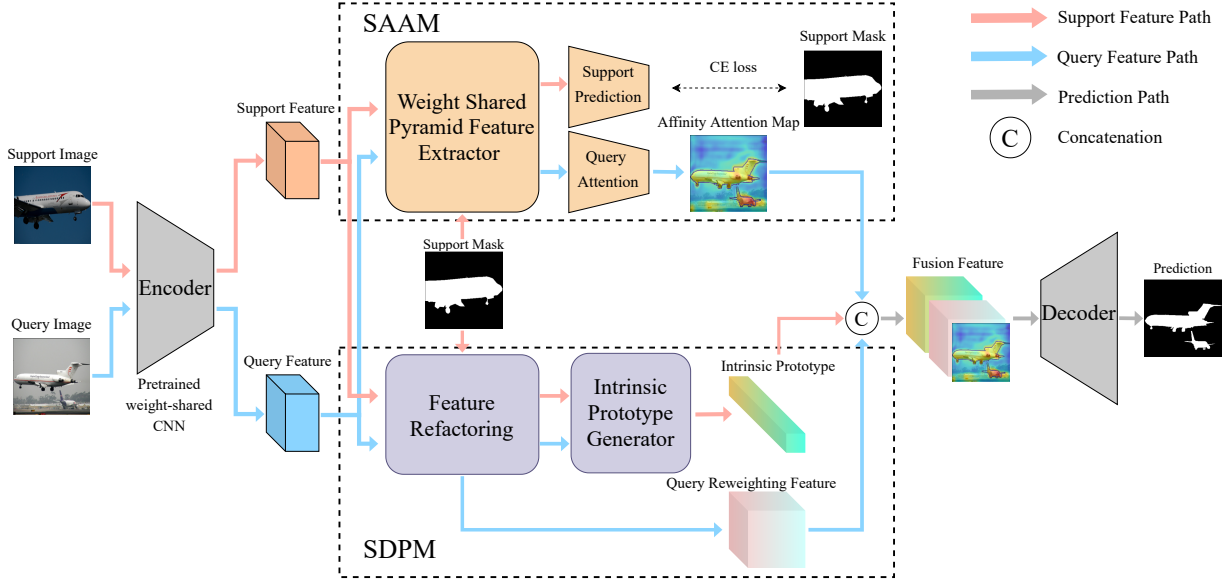


Fig. 3. Structure of SD-AANet. In SD-AANet, middle-level features of CNN backbone and support mask are input to SDPM and SAAM. SDPM uses support prototype to realize channel reweighting on support and query features. Then self-distillation approach in SDPM produces intrinsic support prototype. SAAM introduces support ground truth supervision to a learnable pyramid feature extractor, producing high-quality query attention map. Finally, the fusion of intrinsic prototype, query feature and query attention goes through the decoder to predict the final result.

to enrich query features with the support features. ASGNet [37] introduces the superpixel over-segmentation method into few-shot segmentation and adaptively allocates the generated prototypes to generalize better to unseen classes. SCL [38] design a self-guided and cross-guided learning approach extract more comprehensive support information. SCL and ASGNet achieve the state-of-the-art results on both PASCAL-5<sup>i</sup> and COCO-20<sup>i</sup> for 1-shot and 5-shot segmentation respectively.

### III. PROPOSED METHOD

In this section, we first briefly describe the definition of the few-shot segmentation task in Subsection III-A. Then in Subsection III-B and Subsection III-C, we introduce our self-distillation guided prototype generating module (SDPM) and supervised-based affinity attention module (SAAM) in details respectively. Finally, in Subsection III-D, we discuss our proposed self-distillation embedded affinity attention model (SD-AANet) from a global perspective.

#### A. Problem Setting

Few-shot segmentation is proposed to segment target of unseen classes under the guidance of a few annotated samples of the same classes. The dataset is split to two sets, training set  $D_{train}$  and test set  $D_{test}$ , taking the class as the split standard. Defining the classes in  $D_{train}$  as  $C_{train}$  and the classes in  $D_{test}$  as  $C_{test}$ , the two sets do not intersect, which means  $C_{train} \cap C_{test} = \phi$ .

Training and testing processes of few-shot segmentation can be seen as episodes. The episode paradigm was proposed in [39], and Shaban et al. [9] first introduce it to few-shot segmentation. Each episode is consist of a support set  $S$  and a query set  $Q$  of the same class  $C$ . There are  $K$  samples in the support set  $S$ , which formulated as  $S =$

$\{(I_s^1, M_s^1), (I_s^2, M_s^2), \dots, (I_s^K, M_s^K)\}$ . Each image-label pair  $(I_s^i, M_s^i)$  represent a sample in  $S$ , where  $I_s^i$  and  $M_s^i$  are the support image and its ground truth respectively. Similar to the support set  $S$ , query set  $Q$  has one sample  $(I_q, M_q)$ , where  $I_q$  and  $M_q$  are the query image and its ground truth respectively, having the same class  $C$  with the support set  $S$ . The input of the model is a pair of query image  $I_q$  and support set  $S$ , formulated as  $\{I_q, S\} = \{I_q, (I_s^1, M_s^1), (I_s^2, M_s^2), \dots, (I_s^K, M_s^K)\}$ . Query ground truth  $M_q$  is invisible in training of few-shot segmentation and it is used to evaluate the performance.

#### B. Self-distillation Guided Prototype Generating Module

1) *Inspirations:* Current prototypical learning methods, such as PFENet [36], approach a great performance on PASCAL-5<sup>i</sup> and COCO-20<sup>i</sup>, outperforming previous works by a large margin. Prototypes generated by these methods can efficiently guide the segmentation of query target. However, there is a large feature differences between support and query images. So we need to narrow the gap between support and query features. Objects always have two types of features, intrinsic features which commonly exist in all objects of this class and unique features which may distinct in different objects. Take aeroplane as an example, all aeroplanes are made by metal and have wings. These features existing in all aeroplanes can be seen as intrinsic features. As the differences of shooting angle and lighting conditions, the shape and color of aeroplanes can be different, so these are unique features. In few-shot segmentation, we need to find representative features of support and query images containing abundant intrinsic features.

The knowledge distillation approach proposed by Hinton et al [40] greatly inspires us to transfer the knowledge between the two prototypes. Zagoruyko et al [41] and He et al [42]

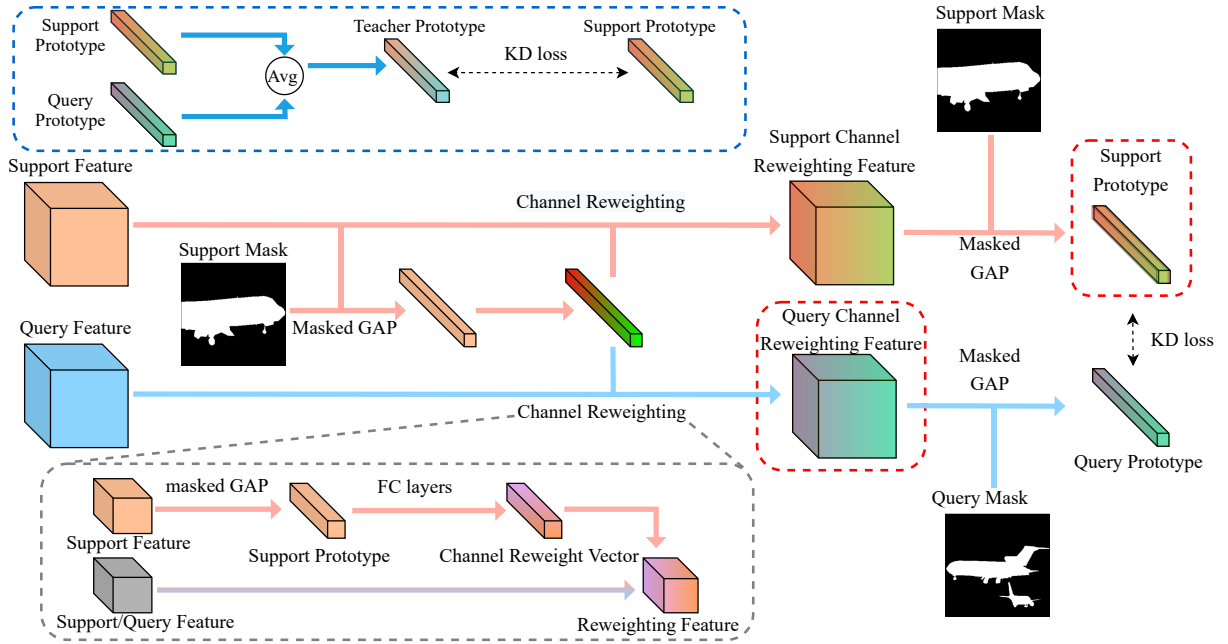


Fig. 4. SDPM first applies masked GAP to generate support prototype, then it uses support prototype to produce channel reweighting vector. Channels of both support feature and query feature are reweighting by above-mentioned reweighting vector. After that, new support prototype and query prototype are generated by masked GAP, then self-distillation approach is used between two prototypes to produce intrinsic support prototype. In order to promote learning process of model, teacher vector in self-distillation approach is the average of support prototype and query prototype, as shown in blue dotted box. The outputs of SDPM are query channel reweighting feature and support prototype shown in red dotted boxes.

expand the knowledge distillation technique by using attentions in middle layers. Fukuda et al [43] proposed integrating multiple teacher networks to teach the student network. Lyu et al [44] realize the knowledge distillation in a single deep neural network, which contains both student network and teacher network.

Otherwise, it is noteworthy that some channels in feature map may not contain object information, having no help for the segmentation. CENet [45] and CBAM [46] make outstanding achievement by designing channel attention methods.

Inspired by the above methods, we introduce self-distillation approach to prototypical learning based method and design a support feature guided channel reweighting operation, extracting intrinsic features and narrowing the gap between support prototype and query prototype.

2) *Support Guided Channel Reweighting*: Different from the SENet [45] which uses global feature to reweight channels of feature map, we alternatively adopt support prototype which is more suitable to get object-related information. As shown in Fig. 4, architecture in gray dotted box is the variation of SE Module. Both support image  $I_s$  and query image  $I_q$  with same class go through a shared backbone CNN, denoted as  $\mathcal{F}(\cdot)$ .  $M_s$  and  $M_q$  denote the ground truth of support and query,  $F_s$  and  $F_q$  denote the support feature and query feature which are outputs of middle-level layers of the backbone CNN:

$$F_s = \mathcal{F}(I_s), F_q = \mathcal{F}(I_q) \quad (1)$$

note that the  $I_s$  and  $I_q$  have same shape  $n \times c \times h \times w$ , in which  $n$ ,  $c$ ,  $h$  and  $w$  represent batch size, number of channels, height and width of the feature map.

Then support prototype is generated by masked GAP, calculating the average vector of the features in object area in feature map:

$$p_s = \mathcal{F}_p(F_s, M_s) = \frac{\sum_{i=1}^h \sum_{j=1}^w F_s^{(i,j)} [M_s^{(i,j)} == 1]}{\sum_{i=1}^h \sum_{j=1}^w [M_s^{(i,j)} == 1]} \quad (2)$$

where  $i$  and  $j$  denote the index of row and column,  $F_s^{(i,j)}$  denotes the position at row  $i$  and column  $j$  in support feature map and  $M_s^{(i,j)}$  denotes the position at row  $i$  and column  $j$  in support ground truth.  $\mathcal{F}_p(\cdot)$  denotes the masked GAP operation. To guarantee the correctness of the Eq. 2,  $M_s$  is resized to the same height and width with the support feature map.  $[\cdot]$  denotes Iverson bracket, a notation that signifies a number that is 1 if the condition in square brackets is satisfied, and 0 otherwise, i.e.

Acquired support prototype is then input to a series of fully connected layers (FC layers) to learn contributions of each feature channel, and there are ReLU function between FC layers. Output of the FC layers is also a vector having same number of channel with support feature and query feature. The whole block is shown in Fig. 5(a) named support SE (SSE) block.  $\mathcal{F}_{CR}(\cdot)$  and  $v_s$  denote the FC layers and output channel reweighting vector respectively, so we have  $v_s = \mathcal{F}_{CR}(p_s)$ .

The channel reweighting vector  $v_s$  scales channels of support feature and query feature, according to each channel's importance. To avoid losing the original information in the feature, we use the average of scaled feature and input feature as the final channel reweighting feature:

$$\tilde{F}_s = \frac{\mathcal{F}_{scale}(v_s, F_s) + F_s}{2}, \tilde{F}_q = \frac{\mathcal{F}_{scale}(v_s, F_q) + F_q}{2} \quad (3)$$



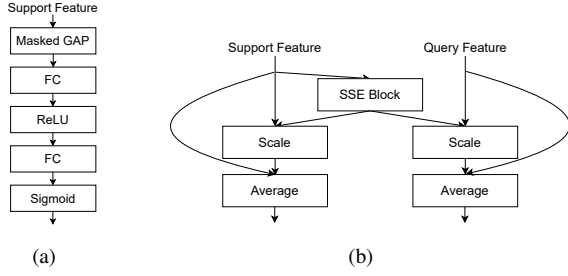


Fig. 5. Support prototype based channel reweighting is designed based on the work of [45]. Support guided Squeeze-and-Excitation (SSE) block (a) applies masked GAP on support feature to generate support prototype, then support prototype goes through FC layers to produce channel reweighting vector, also ReLU and Sigmoid are contained. We use this vector to reweighting channels of support and query features, then the average of reweighting feature and original feature output as the final results.

where  $\mathcal{F}_{scale}(v_s, F_s)$  denotes the channel scale function and  $\tilde{F}_s$  denotes the final channel reweighting feature, so do the  $\mathcal{F}_{scale}(v_s, F_q)$  and  $\tilde{F}_q$ . The whole process of channel reweighting can be seen in Fig. 5(b).

3) *Self-distillation embedded Method*: After Hinton et al [40] first proposed the knowledge distillation in deep learning, many studies [44], [47], [48] have been conducted to let models learning from themselves. This approach is named as self-distillation which aims to promote performance of model without external knowledge input.

Inspired by above works, we introduce self-distillation approach to prototypical neural network, which can significantly improve few-shot segmentation performance by extracting intrinsic support feature.

To apply the self-distillation approach to generate the intrinsic support prototype, query prototype is used as the teacher. Masked GAP is employed to obtain both support prototype and query prototype from channel reweighting features as  $p'_s = \mathcal{F}_p(\tilde{F}_s, M_s)$ ,  $p'_q = \mathcal{F}_p(\tilde{F}_q, M_q)$ , where  $p'_s$  and  $p'_q$  denote the support prototype and query prototype of channel reweighting features.

The query prototype and support prototype are adopted in self-distillation process. Both two prototypes can be seen as a combination of two parts feature, intrinsic feature and unique feature. So  $p'_s$  can be represented as  $p'_s(f_i, f_s)$ , where  $f_i$  and  $f_s$  denote the intrinsic feature and support unique feature respectively. Similarly, query prototype  $p'_q$  can be represented as  $p'_q(f_i, f_q)$ , and  $f_q$  is the query unique feature. Following the knowledge distillation method, we apply the Kullback Leibler (KL) divergence loss to realize the supervision of support prototype:

$$d_s = \text{Softmax}(p'_s), d_q = \text{Softmax}(p'_q) \quad (4)$$

$$L_{KD} = KL(d_t \| d_s) = \sum_{i=1}^c d_t^i \log \frac{d_s^i}{d_t^i} \quad (5)$$

where  $\text{Softmax}(\cdot)$  denotes the softmax function, and  $d_s$  and  $d_q$  denote the outputs of the softmax function while inputs are  $p'_s$  and  $p'_q$ .  $d_t$  denotes the teacher prototype in knowledge distillation operation and equals to  $d_t = \frac{d_s + d_q}{2}$ .  $L_{KD}$  in Eq. 5 denotes the loss of self-distillation between support prototype

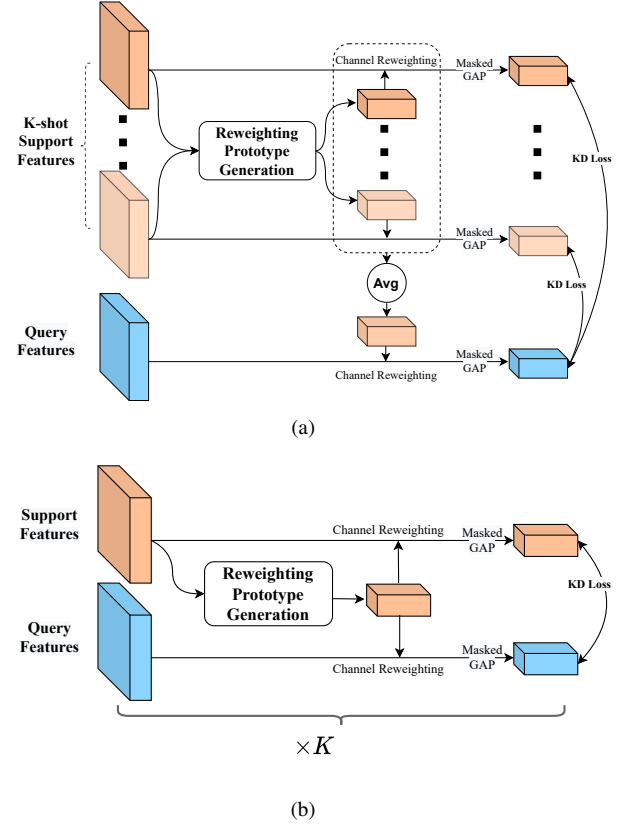


Fig. 6. Two strategies of SDPM in k-shot task, Integral Teacher Prototype Strategy (a) use the average of K reweighting vectors and masked GAP to produce the teacher prototype, while Separate Teacher Prototype Strategy (b) produces a exclusive teacher prototype for each support prototype.

and teacher prototype, and  $KL(\cdot)$  denotes the KL divergence function, which aims to draw support prototype near to teacher prototype.

Self-distillation approach prompts the support prototype to be close to the query prototype. Because the two prototypes are combinations of intrinsic feature and unique feature, the approach results in the lessen of unique feature and strengthen of intrinsic feature, which means  $p'_s(f_i, f_s) \rightarrow p'_s(f_i)$ .  $p'_s(f_i)$  in formula denotes the support prototype with only intrinsic feature, more suitable for guiding the query segmentation.

SDPM can efficiently reduce the unique feature in support prototype and significantly ease the gap between support and query features. Experiments in Section IV-C show the improvement of performance more intuitively.

4) *K-shot Setting*: In addition to 1-shot segmentation, segmenting the query target under the guidance of K (not one) support images is defined as K-shot segmentation. To extend SDPM to K-shot segmentation, this module needs to be modified appropriately. Because of the distinctions between K support images, teacher prototype extracted from query feature should supervises each support prototype separately. Depending on whether the teacher prototypes of K support prototypes are same, we design two strategies of SDPM for K-shot segmentation task, Integral Teacher Prototype Strategy and Separate Teacher Prototype Strategy. Details of two strategies are shown in Fig. 6.

As shown in Fig. 6(a), the core idea of Integral Teacher

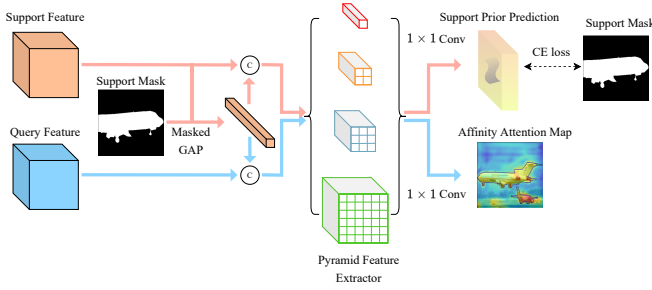


Fig. 7. SAAM produces support prototype using masked GAP and concatenates support prototype to both support feature and query feature. PPM [6] is adopted to extract features of two concatenated results. Then two  $1 \times 1$  convolutions with channel of 1 and 2 are applied to generate support prediction and query attention map. Support ground truth is used to supervise the support prediction, and the output of SAAM is query attention map.

Prototype Strategy is applying the average of  $K$  reweighting vectors to scale each channel of query feature. Then masked GAP is adopted to extract teacher prototype, and  $K$  knowledge distillation losses are calculated between teacher prototype and each support prototype. The final self-distillation loss is the average of  $K$  losses.

$$\tilde{F}_q = \frac{\mathcal{F}_{scale} \left( \sum_{i=1}^K v_s^i, F_q \right) + F_q}{2} \quad (6)$$

$$L_{KD}^I = \frac{1}{K} \sum_{i=1}^K KL(p_q' \| v_s^i) \quad (7)$$

where  $v_s^i$  denotes the prototype of  $i$ -th support sample,  $p_q'$  denotes the query prototype generated from  $\tilde{F}_q$ , and  $L_{KD}^I$  denotes the knowledge distillation loss of Integral Teacher Prototype Strategy.

Separate Teacher Prototype Strategy is shown in Fig. 6(b). Different from Integral Teacher Prototype Strategy, Separate Teacher Prototype Strategy produces an exclusive teacher prototype for each support prototype, via applying each reweighting vector to scale the query feature separately.

$$\tilde{F}_q^i = \frac{\mathcal{F}_{scale}(v_s^i, F_q) + F_q}{2} \quad (8)$$

$$L_{KD}^S = \frac{1}{K} \sum_{i=1}^K KL(p_q^i \| v_s^i) \quad (9)$$

where  $\tilde{F}_q^i$  and  $p_q^i$  denote the query reweighting feature and teacher prototype produced by  $i$ -th support reweighting vector.  $L_{KD}^S$  denotes the knowledge distillation loss of Separate Teacher Prototype Strategy. Final output query feature  $\tilde{F}_q$  of SDPM is the average of  $K$  query reweighting features, formulated as  $\tilde{F}_q = \frac{1}{K} \sum_{i=1}^K \tilde{F}_q^i$ .

No matter which strategy is applied, the final output support prototype is the average of  $K$  support prototypes. The ablation experiments in Section IV-C show the performances of two strategies. In the end, we use Separate Teacher Prototype Strategy in our overall model.

### C. Supervised Affinity Attention Mechanism

1) *Inspiration*: Many works on semantic segmentation and few-shot segmentation introduce various of attention mechanisms. Attention mechanism can effectively capture the location of object and let deep neural network models know where to focus. PGNet [10] uses a graph structure to represent the relationship between pixels of support and query, and produces an attention map of query image which contains spatial information of query target. PFENet [36] uses high-level features of both support and query to generate query attention map. By employing ImageNet [49] pre-trained model as backbone and fixing its weights, the prior attention mechanism is training-free.

However, the ImageNet pre-trained model is produced to tackle the classification task, which is not suitable to generate attention map in few-shot segmentation task straightly. So we propose a supervised affinity attention mechanism (SAAM), which can solve the problem caused by unrepresentative of few support features. The architecture of our SAAM is shown in Fig. 7.

2) *Supervised Attention*: We first utilize masked GAP to obtain support prototype and expand it to the same spatial shape with support feature. Then the expanded prototype is concatenated to both support feature and query feature, we define the results as  $F_{C,s}$  and  $F_{C,q}$  respectively. Following,  $F_{C,s}$  and  $F_{C,q}$  are input to a pyramid feature extractor severally and outputs are defined as  $F_{P,s}$  and  $F_{P,q}$ . We use Pyramid Pooling Module (PPM) [6] as the pyramid feature extractor.

On the head of the PPM, there are two  $1 \times 1$  convolution layers (Convs) to generate support prediction and query attention map respectively. Support prediction is generated by  $1 \times 1$  Conv with two output channels. The  $1 \times 1$  Conv for query attention map generation has only one output channel. Then support label is applied to supervise the SAAM.

$$L_{ce,s} = - \sum_{i=1}^h \sum_{j=1}^w \left( M_s^{(i,j)} \cdot \log \left( P_s^{(i,j)} \right) \right) \quad (10)$$

where  $L_{ce,s}$  is the cross entropy loss of support prediction in SAAM.  $M_s^{(i,j)}$  and  $P_s^{(i,j)}$  are  $(i, j)$  location of support mask and support prediction in SAAM.

3) *K-shot Setting*: K-shot setting of SAAM is intuitive, because the only different part is support path.  $K$  support features go through SAAM severally, then each support prediction is supervised by its own label. Loss of K-shot SAAM is the average of  $K$  losses.

$$L_{ce,s} = \sum_{i=1}^K L_{ce,s}^i \quad (11)$$

where  $L_{ce,s}^i$  is the cross entropy loss of  $i$ -th support image.

### D. Self-Distillation Embedded Supervised Affinity Attention Network

1) *Model Introduction*: Based on the Self-distillation guided Prototype generating Module (SDPM) and Supervised Affinity Attention Module (SAAM), we propose the Self-Distillation Embedded Supervised Affinity Attention Network

TABLE I  
COMPARISON WITH STATE-OF-THE-ART METHODS ON PASCAL-5<sup>i</sup> WITH CLASS mIOU METRIC. BASELINE IN TABLE FOLLOWS THE PFENET [36].

Methods	Backbone	1-shot					5-shot				
		Fold-0	Fold-1	Fold-2	Fold-3	Mean	Fold-0	Fold-1	Fold-2	Fold-3	Mean
OSLSM [9]	VGG-16	33.6	55.3	40.9	33.5	40.8	35.9	58.1	42.7	39.1	44.0
co-FCN [32]	VGG-16	36.7	50.6	44.9	32.4	41.1	37.5	50.0	44.1	33.9	41.4
SG-One [13]	VGG-16	40.2	58.4	48.4	38.4	46.3	41.9	58.6	48.6	39.4	47.1
AMP [50]	VGG-16	41.9	50.2	46.7	34.7	43.4	41.8	55.5	50.3	39.9	46.9
PANet [35]	VGG-16	42.3	58.0	51.1	41.2	48.1	51.8	64.6	59.8	46.5	55.7
PGNet [10]	ResNet50	56.0	66.9	50.6	50.4	56.0	57.7	68.7	52.9	54.6	58.5
FWB [17]	ResNet101	51.3	64.5	56.7	52.2	56.2	54.8	67.4	62.2	55.3	59.9
CANet [14]	ResNet50	52.5	65.9	51.3	51.9	55.4	55.5	67.8	51.9	53.2	57.1
CRNet [51]	ResNet50	-	-	-	-	55.7	-	-	-	-	58.8
RPMs [15]	ResNet50	55.2	65.9	52.6	50.7	56.3	56.3	67.3	54.5	51.0	57.3
SimPropNet [52]	ResNet50	54.8	67.3	54.5	52.0	57.2	57.2	68.5	58.4	56.1	60.0
PPNet [53]	ResNet50	47.8	58.8	53.8	45.6	51.5	58.4	67.8	64.9	56.7	62.0
DAN [12]	ResNet101	54.7	68.6	57.8	51.6	58.2	57.9	69.0	60.1	54.9	60.5
PFENet [36]	ResNet50	61.7	69.5	55.4	56.3	60.8	63.1	70.7	55.8	57.9	61.9
ASGNet [37]	ResNet101	59.8	67.4	55.6	54.4	59.3	64.6	71.3	<b>64.2</b>	57.3	64.4
SCL [38]	ResNet50	<b>63.0</b>	70.0	56.5	<b>57.7</b>	<b>61.8</b>	64.5	70.9	57.3	58.7	62.9
Baseline(ours)	ResNet50	59.5	70.0	55.9	56.1	60.4	63.7	70.5	57.2	57.5	62.2
SD-AANet(ours)	ResNet50	60.9	<b>70.8</b>	58.4	57.3	61.9	<b>65.5</b>	<b>71.6</b>	62.5	<b>62.3</b>	<b>65.5</b>

(SD-AANet) as shown in Fig. 3. Encoder of SD-AANet is ImageNet [49] pre-trained CNN with fixed model weights, and output features of both support image and query image are go through  $1 \times 1$  convolutions to reduce the number of channels to 256 as PFENet [36].

Self-distillation guided Prototype generating Module (SDPM) and Supervised Affinity Attention Module (SAAM) are placed after  $1 \times 1$  convolutions. SDPM, as shown in Fig. 4, applies channel reweighting and self-distillation approach to extract intrinsic prototype. Channel reweighting helps to restrain the channels of background feature and enhance channels of foreground feature. Self-distillation approach adopts query prototype to teach support prototype, which significantly eases the gap between support and query features. The intrinsic support prototype can realize higher-quality query segmentation. SAAM introduces support predict supervision to a learnable CNN-based architecture, obtaining a query attention map based on affinity between support and query with same class, as shown in Fig. 7.

In K-shot setting, we design two strategies for SDPM. Details of two strategies are shown in Fig. 6. For SAAM, approach in K-shot setting is to straightly supervise each support samples.

2) *Loss Function Definition*: For the whole model, we choose cross entropy loss  $L_{ce}$  for the final segmentation prediction. Counting losses of SDPM and SAAM in, the total loss of SD-AANet is combination of  $L_{ce}$ ,  $L_{KD}$  and  $L_{ce,s}$  as

$$L = L_{ce} + \alpha \cdot L_{KD} + \beta \cdot L_{ce,s} \quad (12)$$

where  $\alpha$  and  $\beta$  are coefficients of  $L_{KD}$  and  $L_{ce,s}$ , whose propose are balance three loss compositions.

## IV. EXPERIMENTS

### A. Implementation Details

1) *Datasets*: The datasets of PASCAL-5<sup>i</sup> [9] and COCO-20<sup>i</sup> [16], [17] are used in experiments to evaluate our method. PASCAL-5<sup>i</sup> consists of two parts, PASCAL VOC 2012 [54] and extended annotations from SDS datasets [55]. There are 20 classes in original PASCAL VOC 2012 and SDS, and they are evenly divided into 4 folds, defined as Fold- $i$ ,  $i \in \{0, 1, 2, 3\}$ . Each fold contains 5 classes following settings in OSLSM [9], and 1000 pairs of support-query are used in our test.

Following [17], COCO dataset, owns 80 classes totally, is also splited into 4 folds with 20 classes in each fold. The set of class indexes contained in fold- $i$  is written as  $\{4x - 3 + i\}$ ,  $i \in \{1, 2, \dots, 20\}$ . Due to the number of images in COCO validation is 40137, which is much more than the PASCAL-5<sup>i</sup>. So we randomly choose 4000 support-query pairs on each fold during testing following [17], which can provide more reliable and stable results for 20 classes than 1000 pairs.

To realize the few-shot segmentation, we use three folds to train the model and test the model on last fold for cross-validation. We alternatively choose different fold in testing to evaluate performance of our model, and we carry out five rounds of experiment and take the average to get the final experimental results.

2) *Experimental Setting*: We use PyTorch to construct our framework, and we apply ResNet50 and ResNet101 [18] as our backbones for PASCAL-5<sup>i</sup> and COCO-20<sup>i</sup> respectively. We choose the ResNet with atrous convolutions as previous works [14], [17], [56]. The ImageNet [49] pretrained weights provided by PyTorch are used to initialize backbone networks. We use SGD as our optimizer. We set the momentum and weight decay to 0.9 and 0.0001 respectively. The 'poly' policy [5] is adopted in our experiments to decay the learning rate by multiplying  $\left(1 - \frac{\text{current\_iter}}{\text{max\_iter}}\right)^{\text{power}}$  where *power* is set to 0.9.

TABLE II

COMPARISON WITH STATE-OF-THE-ART METHODS ON COCO-20<sup>i</sup> WITH CLASS mIoU METRIC. BASELINE IN TABLE FOLLOWS THE PFENET [36]. MODELS WITH † ARE EVALUATED ON THE LABELS RESIZED TO 473 × 473 SIZE. MODELS WITHOUT † ARE TESTED ON LABELS WITH THE ORIGINAL SIZES.

Methods	Bcakbone	1-shot					5-shot				
		Fold-0	Fold-1	Fold-2	Fold-3	Mean	Fold-0	Fold-1	Fold-2	Fold-3	Mean
FWB [17]	ResNet101	19.9	18.0	21.0	28.9	21.2	19.1	21.5	23.9	30.1	23.7
PANet [35]	VGG-16	-	-	-	-	20.9	-	-	-	-	29.7
DAN [12]	ResNet101	-	-	-	-	24.4	-	-	-	-	29.6
RPMs [15]	ResNet50	-	-	-	-	30.6	-	-	-	-	35.5
PPNet [53]	ResNet50	28.1	30.8	29.5	27.7	29.0	39.0	40.8	37.1	37.3	38.5
PFENet [36]	ResNet101	34.3	33.0	32.3	30.1	32.4	38.5	38.6	38.2	34.3	37.4
PFENet† [36]	ResNet101	36.8	41.8	38.7	36.7	38.5	40.4	46.8	43.2	40.5	42.7
ASGNet [37]	ResNet50	-	-	-	-	34.6	-	-	-	-	42.5
SCL [38]	ResNet101	36.4	38.6	37.5	35.4	37.0	38.9	40.5	41.5	38.7	39.9
Baseline(ours)	ResNet101	35.5	41.5	37.6	36.1	37.7	41.5	47.3	45.2	41.6	43.9
Baseline(ours)†	ResNet101	36.7	41.9	38.1	37.2	38.5	41.7	48.6	46.8	42.9	45.0
SD-AANet(ours)	ResNet101	39.3	43.9	39.8	39.5	40.6	43.1	51.4	52.7	46.3	48.4
SD-AANet(ours)†	ResNet101	<b>39.6</b>	<b>44.3</b>	<b>39.9</b>	<b>39.9</b>	<b>40.9</b>	<b>43.2</b>	<b>51.9</b>	<b>52.9</b>	<b>46.6</b>	<b>48.7</b>

$\alpha$  and  $\beta$  are set to 50 and 0.5 respectively. We use PFENet [36] as our baseline.

The experiments on PASCAL-5<sup>i</sup> train models for 200 epochs as [36], while the learning rate and batch size are set to 0.0025 and 4. Because there are more images in training set of COCO-20<sup>i</sup>, we train models for 50 epochs with 0.0005 and 8 for learning rate and batch size respectively. We fix the parameters of backbone networks and update other parameters during training. Each example is processed with mirror operation and random rotation from -10 to 10 degrees. Finally, limited by equipment performance, we randomly crop 321 × 321 patches from the processed images as training samples, which significantly reduces storage consumption and runtime. During evaluation, we resize the processed images to 321 × 321 and pad zero to maintain the original aspect ratio of images. Then the prediction is resized back to original label sizes to evaluate performance. Following [36], for COCO-20<sup>i</sup>, we also resize the prediction to 473 × 473 with respect to its original aspect ratio to make another evaluation. The single-scale results are output without multi-scale testing and any other post-processing. Our experiments are conducted on an NVIDIA GeForce RTX3060 GPU and Intel Xeon CPU 10900K. The code will be made publicly available soon.

3) *Evaluation Metrics*: Following [14], [17], [36], we adopt class mean intersection over union (mIoU) as our evaluation metric for ablation study, because the class mIoU is more reasonable than the foreground-background IoU (FB-IoU) [14]. The formulation of class mIoU is  $\frac{1}{C} \sum_{i=1}^C IoU_i$ , where  $C$  is the number of classes belong to each fold. So  $C = 5$  for PASCAL-5<sup>i</sup> and  $C = 20$  for COCO-20<sup>i</sup>. The  $IoU_i$  is intersection over union of  $i$ -th class.

## B. Results

As shown in Tables I and II, we adopt ResNet50 and ResNet101 to build our models for PASCAL-5<sup>i</sup> and COCO-20<sup>i</sup> respectively. And we report the class mIoU results to prove the performance of our proposed models. By incorporating the SDPM and SAAM, with the 321 × 321 size of input images

which is smaller than 473 × 473 used in previous works, our SD-AANet still achieves comparable state-of-the-art results on PASCAL-5<sup>i</sup> and reaches new state-of-the-art results on COCO-20<sup>i</sup> for class mIoU metric.

In Table I, we compare our model with other state-of-the-art methods on PASCAL-5<sup>i</sup>. It can be seen that SD-AANet reaches comparable state-of-the-art results for both 1-shot and 5-shot tasks. For 1-shot task, SD-AANet achieves competitive performance with class mIoU increases of 1.1% and 2.6% for PFENet [36] and ASGNet [37], comparable with SCL [38]. For 5-shot task, SD-AANet achieves significant results with class mIoU increases of 2.6% and 1.1% for SCL [38] and ASGNet [37]. Our SD-AANet improve the performance with 1.5% and 3.3% rise on class mIoU than our baseline, which do not have SDPM and SAAM.

Table II shows the comparison between our SD-AANet and other state-of-the-art methods on COCO-20<sup>i</sup>. Our SD-AANet is far superior to other methods, with class mIoU gains of 2.4% and 6.0% for 1-shot and 5-shot tasks respectively. The class mIoU results also increases 2.4% and 3.7% than our baseline.

## C. Ablation Study

1) *Ablation Study of SDPM and SAAM*: To quantitatively analyze the influence of SDPM and SAAM, we conduct an experiment about the performance of model w/ and w/o the SDPM and SAAM. Table III shows the class mIoU results of each model on PASCAL-5<sup>i</sup> for 1-shot task.

TABLE III  
ABLATION STUDY OF OUR PROPOSED SDPM AND SAAM ON PASCAL-5<sup>i</sup> FOR 1-SHOT SEGMENTATION. “SD-AANet” MEANS THE MODEL WITH BOTH SDPM AND SAAM.

Methods	Fold-0	Fold-1	Fold-2	Fold-3	Mean
Baseline	59.5	70.0	55.9	56.1	60.4
Baseline + SAAM	59.7	70.4	56.7	56.4	60.8
Baseline + SDPM	60.3	70.2	57.7	57.2	61.4
SD-AANet	<b>60.9</b>	<b>70.8</b>	<b>58.4</b>	<b>57.3</b>	<b>61.9</b>



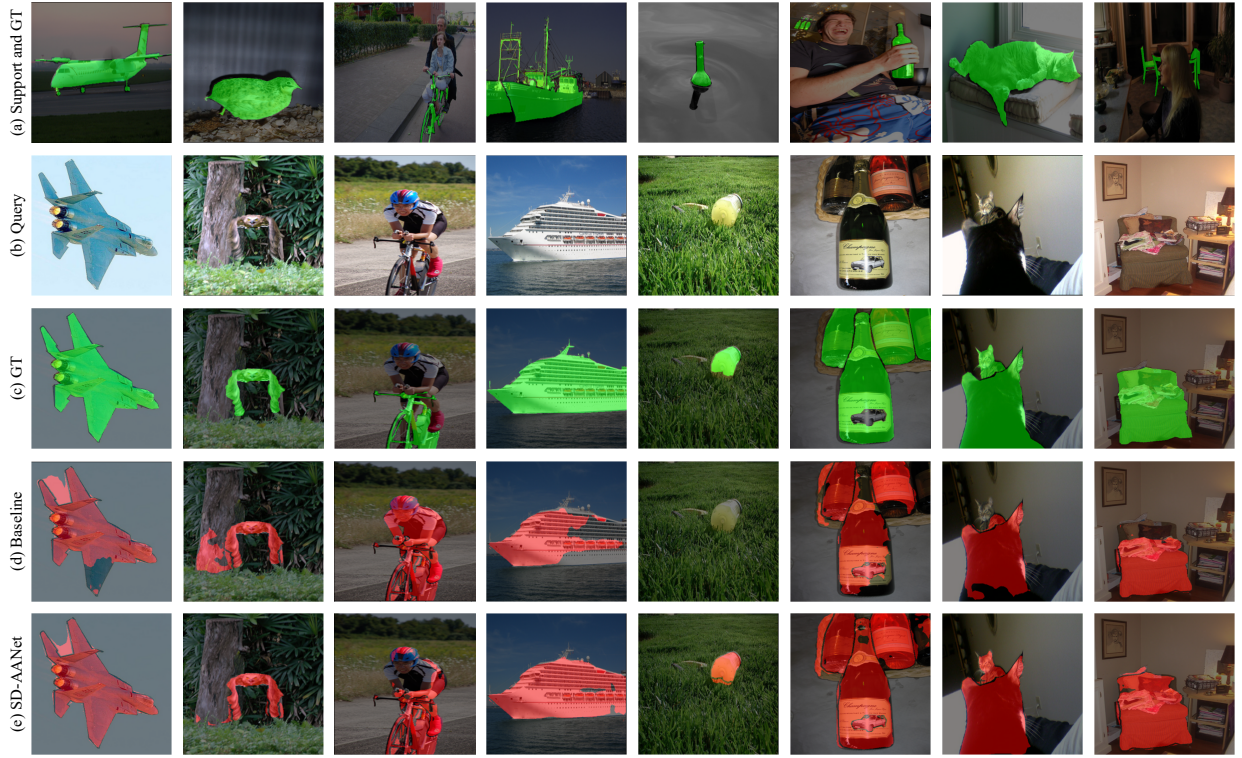


Fig. 8. Qualitative results of the proposed SD-AANet and the baseline. The results is produced on PASCAL-5<sup>i</sup> of 1-shot segmentation. From top to bottom: (a) support image and its ground truth, (b) query image, (c) ground truth of query image, (d) prediction of baseline, (e) prediction of SD-AANet.

It can be seen in Table III that, compared to baseline, using only SAAM and SDPM improves the performance with class mIoU increases of 0.4% and 1.0% respectively. Adopting both SAAM and SDPM can further improve the performance, with 1.5% class mIoU gain.

TABLE IV

ABLATION STUDY OF USING SINGLE-SCALE INFERENCE OR MULTI-SCALE INFERENCE ON PASCAL-5<sup>i</sup> FOR 1-SHOT SEGMENTATION.

Methods	Fold-0	Fold-1	Fold-2	Fold-3	Mean
Single-scale Inference	<b>60.9</b>	70.8	58.4	57.3	61.9
Multi-scale Inference	60.8	<b>70.9</b>	<b>59.3</b>	<b>57.8</b>	<b>62.2</b>

2) *Ablation Study of Multi-scale Inference*: Table IV shows a comparison experiment between single-scale inference and multi-scale inference of SD-AANet. The experiment is conducted on PASCAL-5<sup>i</sup> for 1-shot task. In this experiment, we resize the logits before classify layer to  $321 \times 321$  and  $473 \times 473$ , and adopting softmax operation to get two prediction with different size. Then we resize the  $321 \times 321$  prediction to  $473 \times 473$  by using bilinear interpolation. Finally the two  $473 \times 473$  predictions are added to get final prediction. The result shows that multi-scale inference can improve the performance slightly with 0.3% class mIoU gain.

3) *Ablation Study of 5-shot Strategy*: Table V studies the influence of different 5-shot strategy of SDPM. As discussed in Section IV-C, we design two strategies for SDPM in 5-shot task, Integral Teacher Prototype Strategy and Separate Teacher Prototype Strategy, which named Integral Strategy and Separate Strategy as next. Comparison experiment shown in Table V indicates the Separate Strategy achieves more

TABLE V  
ABLATION STUDY OF SDPM WITH INTEGRAL TEACHER PROTOTYPE STRATEGY OF SEPARATE TEACHER PROTOTYPE STRATEGY ON PASCAL-5<sup>i</sup> FOR 5-SHOT SEGMENTATION.

Methods	Fold-0	Fold-1	Fold-2	Fold-3	Mean
Integral Strategy	64.3	70.8	<b>61.7</b>	58.8	63.9
Separate Strategy	<b>65.5</b>	<b>71.6</b>	<b>62.5</b>	<b>62.3</b>	<b>65.5</b>

outstanding result than Integral Strategy. It means that assign a unique teacher prototype to each support prototype can facilitate the production of intrinsic support prototype, which promotes the segmentation performance of query target.

#### D. Visualization Analysis

1) *Qualitative Visualization of Segmentation Results*: To show the performance of our proposed architectures intuitively, we visualize final prediction masks produced by our SD-AANet in Fig. 8. Meanwhile, we compare the segmentation results between baseline and SD-AANet to evaluate the performance improvement realized by SD-AANet.

As shown in Fig. 8, the first row is support image and its ground truth, which is marked in green in figures. The second row is query image and the third row is the ground truth of it, which is also marked in green. The fourth row is the prediction result of baseline, and the fifth row is the prediction of SD-AANet, marked in red.

As we can see in the first column in Fig. 8, the plane is a large-scale object with complex feature. The baseline failed to precisely segment one of its aerofoils, and the baseline

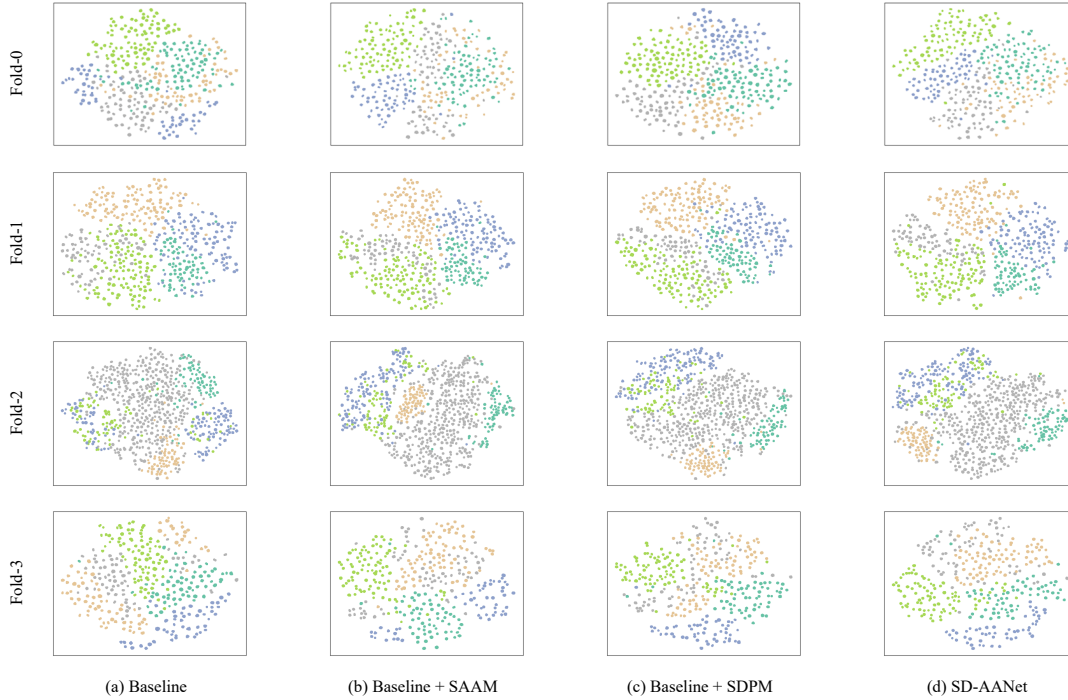


Fig. 9. Visualization comparison study of support prototypes between t-SNE results. Each figure contains 5000 support prototypes generated from the same 5000 image pairs.

mistakenly regards the sky as part of the aeroplane because of the similarity in color between the two objects. But our SD-AANet segments the aeroplane correctly and reduces the area of wrong segmentation significantly. The same results can be seen in next three columns. SD-AANet successfully avoids to segment backgrounds, which have similar feature with the target class, as shown in the second and third columns, although the tree in second query image is very similar to the bird. In the fourth column, the boat has large size and multiple parts with their features abundant of significant differences, such as gunwale, porthole and mast. Faced with so many difficulties, our SD-AANet still can produce more precise prediction than baseline.

The last four columns in Fig. 8 show cases which have tremendous differences between support objects and query target. Taking the fifth column as an example, the bottles in support image and query image has totally different colors, shapes and perspectives, which leads to the segmentation failure of baseline. Relying upon the intrinsic feature extracted by SD-AANet, we can capture intrinsic features of the class and ignore the interference of other factors, so we successfully segment the bottle with negligible error. Cases in the last three columns also confirms this point. Although the case in the sixth column shows our SD-AANet makes mistake to segment the car as bottle, we consider the car is stamped on the bottle which is an understandable mistake, because humans would think it belonged to the bottle in this case.

2) *t-SNE Visualization of Support Prototypes*: We conduct a t-distributed stochastic neighbor embedding (t-SNE) visualization experiment for support prototypes in Fig. 9, which is related to Section IV-C1. In Fig. 9, four columns

in turn represent results of baseline, baseline with SAAM, baseline with SDPM and SD-AANet, and four rows in turn represent four folds from Fold-0 to Fold-3. We use models to process 5000 samples of 5 novel classes and get 5000 support prototypes output from SDPM or backbone. Then t-SNE is adopted to embed prototypes to 2-dimensional space to visualize, and the operation is repeated for 4 methods on 4 folds. As shown in Fig. 9, SDPM can significantly expand the distance between prototypes of different classes and make prototypes of same classes more compact, so the results in columns (c) and (d) are more distinct. The columns (b) and (d) show SAAM can also make support prototypes more discriminative to a certain extent.

Take Fold-1 and Fold-3 as examples, figures about two folds in first column show prototypes of 5 classes mix together and some classes are split at both ends of figures. The second column, which represent baseline with SAAM can distinguish classes slightly clearer, such as grey points in Fold-1 and orange points in Fold-3. In the third column, baseline with SDPM has greater performance to produce intrinsic prototype, so the points with same color seemed more compact such as grey points in Fold-1 and blue points in Fold-3. Combine the SAAM and SDPM, SD-AANet achieve the best performance which can obviously seen in figures. Clear dividing lines can be seen in the fourth column figures of Fold-1 and Fold-3.

3) *Visualization of Performance on Small Target*: To further analyze the segmentation performance of SD-AANet for small targets, we choose the samples whose targets have less than 5000 pixels to conduct comparison experiment between SD-AANet and baseline. The samples are split to 10 parts, each part has a span of 500 pixels. We calculate the average



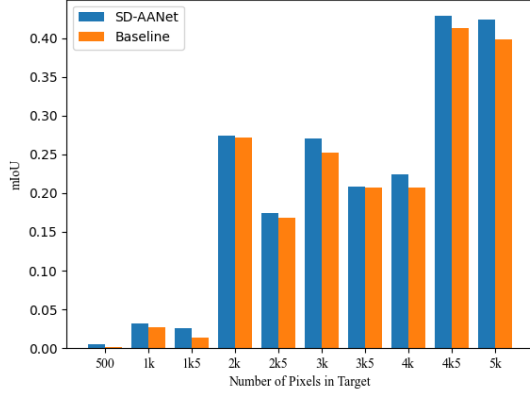


Fig. 10. Quantitative comparative experiment of segmentation performance on small-scale target between baseline and SD-AANet on PASCAL-5<sup>i</sup> for 1-shot segmentation.

class mIoU of each part produced by two models to draw a histogram, shown in Fig. 10.

The results shown in Fig. 10 illustrate that our SD-AANet achieves more class mIoU in all 10 parts, so SD-AANet has greater segmentation performance than baseline for small target segmentation.

4) *Visualization of Affinity Attention*: To intuitively analyze the quality of affinity attention produced by SAAM, we visualize the attention map as shown in Fig. 11. The first two rows are query image and its ground truth label respectively, and the third row is affinity attention map where close to red (warm-toned) means more attention, vice versa.

In first three columns, we can see that SAAM can effectively capture the spatial information of targets, even if they are small or there are multiple targets in one image. The last two columns show the SAAM can focus on large-scale targets and capture key information of separate parts, such as the rearview mirror of the bus and wheels of the aeroplane, with only one support sample.

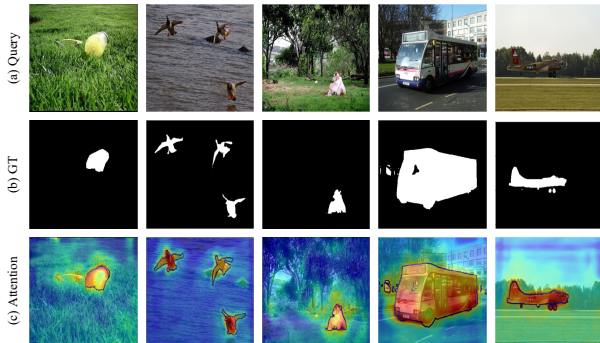


Fig. 11. Visualization of affinity attention map generated by SAAM on PASCAL-5<sup>i</sup> for 1-shot segmentation.

5) *Visualization of Prototype's Representative*: To discuss the representative of support prototype, we calculate the cosine similarity between support prototype and its feature map

$$\cos(x_{i,j}, p'_s) = \frac{x_{i,j}^T \cdot p'_s}{\|x_{i,j}\| \cdot \|p'_s\|} \quad (13)$$

where  $x_{i,j}$  denotes the vector in support feature at  $(i, j)$  location and  $x_{i,j}^T$  denotes its transpose.  $p'_s$  denotes the support prototype output from SDPM. Finally the  $\|\cdot\|$  denotes the norm of the vector.

Similar to attention maps in Fig. 11, the similarity map shown in Fig. 12 use warm-toned color to represent high similarity. Three rows from top to bottom in turn illustrate support image and its ground truth, similarity map produced by baseline and similarity map produced by SA-AANet. In first four columns we can see the prototype produced by SD-AANet can filter more irrelevant background compared to baseline, which means the prototype focus on intrinsic feature to capture the target regardless of other environmental factors. In fifth column, baseline fails to found part of sheep which is mixed up with the fence, while SD-AANet finds the whole spatial area of the sheep.

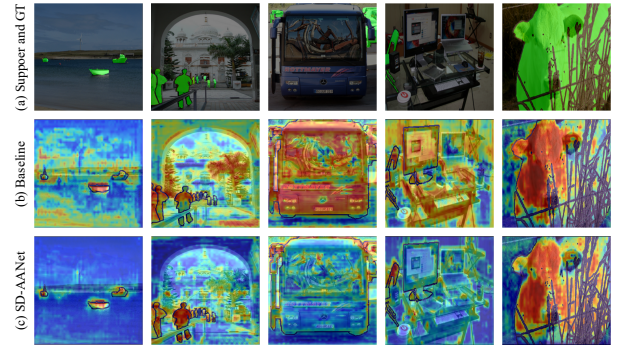


Fig. 12. Visualization of support similarity map generated by support prototype and support feature using cosine similarity. The comparison visualization study is process on PASCAL-5<sup>i</sup> for 1-shot segmentation.

6) *Visualization of Failure Cases*: As shown in Fig. 13, SD-AANet still fails to segment some targets because the target size is too small or the target is very similar to the background. The first column is support image and its ground truth, and the next two columns are query image and its ground truth respectively. The fourth column is attention map produced by SAAM and the last column is prediction of SD-AANet.

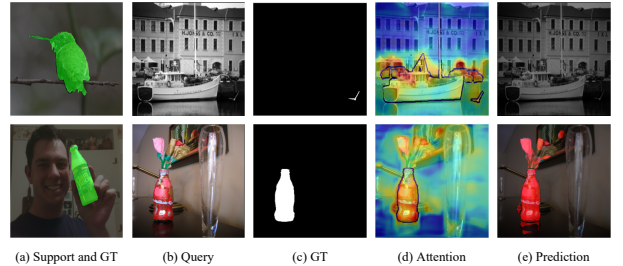


Fig. 13. Visualization study of failure cases of SD-AANet on PASCAL-5<sup>i</sup> for 1-shot segmentation.

We can see in the first row that the target is a bird of very small size, and there are great differences between support object and query target. In second row, the bottle is very similar to the flower which is hard to discriminate. So SD-AANet still not enough to deal with extremely difficult samples.

## V. CONCLUSION

In this paper, we propose a novel few-shot segmentation method named SD-AANet. Our method differs significantly from existing methods in which we realize a novel combination of self distillation learning and small sample segmentation. To address the intra-class variation problem, we propose a self-distillation guided prototype module (SDPM) to extract intrinsic prototype, which can efficiently guide segmentation on query image. We further construct a supervised affinity attention module (SAAM) for generating high quality prior attention map of query image. Extensive experiments verify the performance superiority of our proposed method over the existing state-of-the-art few-shot segmentation methods on two standard benchmarks. Besides, future work may focus on utilizing self distillation to zero-shot segmentation task.

## ACKNOWLEDGMENT

This work was supported by National Natural Science Foundation of China under Grants 62002005 and 62072021.

## REFERENCES

- [1] Jonathan Long, Evan Shelhamer, and Trevor Darrell. Fully convolutional networks for semantic segmentation. In *Proc. IEEE Conf. Comput. Vision Pattern Recognit.*, June 2015.
- [2] Vijay Badrinarayanan, Alex Kendall, and Roberto Cipolla. Segnet: A deep convolutional encoder-decoder architecture for image segmentation. *IEEE Trans. Pattern Anal. Mach. Intell.*, 39(12):2481–2495, 2017.
- [3] Olaf Ronneberger, Philipp Fischer, and Thomas Brox. U-net: Convolutional networks for biomedical image segmentation. In *International Conference on Medical image computing and computer-assisted intervention*, pages 234–241. Springer, 2015.
- [4] Guosheng Lin, Anton Milan, and Chunhua Shen *et al.* Refinenet: Multi-path refinement networks for high-resolution semantic segmentation. In *Proc. IEEE Conf. Comput. Vision Pattern Recognit.*, pages 1925–1934, 2017.
- [5] Liang-Chieh Chen, George Papandreou, and Iasonas Kokkinos *et al.* Deeplab: Semantic image segmentation with deep convolutional nets, atrous convolution, and fully connected crfs. *IEEE Trans. Pattern Anal. Mach. Intell.*, 40(4):834–848, 2017.
- [6] Hengshuang Zhao and Jianping Shi *et al.* Pyramid scene parsing network. In *Proc. IEEE Conf. Comput. Vision Pattern Recognit.*, pages 2881–2890, 2017.
- [7] Tianyi Zhang, Guosheng Lin, and Jianfei Cai *et al.* Decoupled spatial neural attention for weakly supervised semantic segmentation. *IEEE Trans. Multimed.*, 21(11):2930–2941, 2019.
- [8] Lei Zhou, Chen Gong, and Zhi Liu *et al.* SAL: selection and attention losses for weakly supervised semantic segmentation. *IEEE Trans. Multimed.*, 23:1035–1048, 2021.
- [9] Amirreza Shaban, Shray Bansal, and Zhen Liu *et al.* One-shot learning for semantic segmentation. In *British Machine Vision Conference 2017*. BMVA Press, 2017.
- [10] Chi Zhang, Guosheng Lin, and Fayao Liu *et al.* Pyramid graph networks with connection attentions for region-based one-shot semantic segmentation. In *Proc. IEEE Int. Conf. Comput. Vision*, pages 9587–9595, 2019.
- [11] Xianghui Yang, Bairun Wang, and Xinchu Zhou *et al.* Brinet: Towards bridging the intra-class and inter-class gaps in one-shot segmentation. In *British Machine Vision Conference 2020*. BMVA Press, 2020.
- [12] Haochen Wang, Xudong Zhang, and Yutao Hu *et al.* Few-shot semantic segmentation with democratic attention networks. In *Proc. Eur. Conf. Comput. Vision*, volume 12358 of *Lecture Notes in Computer Science*, pages 730–746. Springer, 2020.
- [13] Xiaolin Zhang, Yunchao Wei, and Yi Yang *et al.* Sg-one: Similarity guidance network for one-shot semantic segmentation. *IEEE transactions on cybernetics*, 50(9):3855–3865, 2020.
- [14] Chi Zhang, Guosheng Lin, and Fayao Liu *et al.* Canet: Class-agnostic segmentation networks with iterative refinement and attentive few-shot learning. In *Proc. IEEE Conf. Comput. Vision Pattern Recognit.*, pages 5217–5226, 2019.
- [15] Boyu Yang, Chang Liu, and Bohao Li. Prototype mixture models for few-shot semantic segmentation. In *Proc. Eur. Conf. Comput. Vision*, pages 763–778. Springer, 2020.
- [16] Tsung-Yi Lin, Michael Maire, and Serge J. Belongie *et al.* Microsoft COCO: common objects in context. In *Proc. Eur. Conf. Comput. Vision.*, volume 8693 of *Lecture Notes in Computer Science*, pages 740–755. Springer, 2014.
- [17] Khoi Nguyen and Sinisa Todorovic. Feature weighting and boosting for few-shot segmentation. In *Proc. IEEE Int. Conf. Comput. Vision*, pages 622–631, 2019.
- [18] Kaiming He, Xiangyu Zhang, and Shaoqing Ren *et al.* Deep residual learning for image recognition. In *Proc. IEEE Conf. Comput. Vision Pattern Recognit.*, pages 770–778. IEEE Computer Society, 2016.
- [19] Kaiming He, Xiangyu Zhang, and Shaoqing Ren *et al.* Identity mappings in deep residual networks. In Bastian Leibe, Jiri Matas, Nicu Sebe, and Max Welling, editors, *Proc. Eur. Conf. Comput. Vision*, volume 9908, pages 630–645. Springer, 2016.
- [20] Liang-Chieh Chen, George Papandreou, and Iasonas Kokkinos *et al.* Semantic image segmentation with deep convolutional nets and fully connected crfs. In Yoshua Bengio and Yann LeCun, editors, *Proc. Int. Conf. Learn. Representations*, 2015.
- [21] Liang-Chieh Chen, Yukun Zhu, and George Papandreou *et al.* Encoder-decoder with atrous separable convolution for semantic image segmentation. In Vittorio Ferrari, Martial Hebert, Cristian Sminchisescu, and Yair Weiss, editors, *Proc. Eur. Conf. Comput. Vision*, volume 11211, pages 833–851. Springer, 2018.
- [22] Hengshuang Zhao, Yi Zhang, and Shu Liu *et al.* Pscanet: Point-wise spatial attention network for scene parsing. In *Proc. Eur. Conf. Comput. Vision*, volume 11213 of *Lecture Notes in Computer Science*, pages 270–286. Springer, 2018.
- [23] Jun Fu, Jing Liu, and Haijie Tian *et al.* Dual attention network for scene segmentation. In *Proc. IEEE Conf. Comput. Vision Pattern Recognit.*, pages 3146–3154. Computer Vision Foundation / IEEE, 2019.
- [24] Zilong Huang, Xinggang Wang, and Lichao Huang *et al.* Ccnet: Criss-cross attention for semantic segmentation. In *Proc. IEEE Int. Conf. Comput. Vision*, pages 603–612. IEEE, 2019.
- [25] Gregory Koch, Richard Zemel, and Ruslan Salakhutdinov. Siamese neural networks for one-shot image recognition. In *Proc. Int. Conf. Mach. Learn.*, volume 2, 2015.
- [26] Vinyals Oriol, Blundell Charles, and Lillicrap Timothy *et al.* Matching networks for one shot learning. In *Proc. Adv. Neural Inf. Process. Syst.*, pages 3630–3638, 2016.
- [27] Adam Santoro, Sergey Bartunov, and Matthew Botvinick *et al.* Meta-learning with memory-augmented neural networks. In *Proc. Int. Conf. Mach. Learn.*, volume 48 of *JMLR Workshop and Conference Proceedings*, pages 1842–1850. JMLR.org, 2016.
- [28] Sachin Ravi and Hugo Larochelle. Optimization as a model for few-shot learning. In *Proc. Int. Conf. Learn. Representations*. OpenReview.net, 2017.
- [29] Chelsea Finn, Pieter Abbeel, and Sergey Levine. Model-agnostic meta-learning for fast adaptation of deep networks. In *Proc. Int. Conf. Mach. Learn.*, volume 70 of *Proceedings of Machine Learning Research*, pages 1126–1135. PMLR, 2017.
- [30] Eleni Triantafillou, Tyler Zhu, and Vincent Dumoulin *et al.* Meta-dataset: A dataset of datasets for learning to learn from few examples. In *Proc. Int. Conf. Learn. Representations*. OpenReview.net, 2020.
- [31] Sergi Caelles, Kevis-Kokitsi Maninis, and Jordi Pont-Tuset *et al.* One-shot video object segmentation. In *2017 IEEE Conference on Computer Vision and Pattern Recognition, CVPR 2017, Honolulu, HI, USA, July 21-26, 2017*, pages 5320–5329. IEEE Computer Society, 2017.
- [32] Kate Rakelly, Evan Shelhamer, and Trevor Darrell *et al.* Conditional networks for few-shot semantic segmentation. In *Proc. Int. Conf. Learn. Representations*. OpenReview.net, 2018.
- [33] Nanqing Dong and Eric P. Xing. Few-shot semantic segmentation with prototype learning. In *British Machine Vision Conference 2018, BMVC 2018, Newcastle, UK, September 3-6, 2018*, page 79. BMVA Press, 2018.
- [34] Tao Hu, Pengwan Yang, and Chiliang Zhang *et al.* Attention-based multi-context guiding for few-shot semantic segmentation. In *AAAI*, pages 8441–8448. AAAI Press, 2019.
- [35] Kaixin Wang, Jun Hao Liew, and Yingtian Zou *et al.* Panet: Few-shot image semantic segmentation with prototype alignment. In *Proc. IEEE Int. Conf. Comput. Vision*, pages 9197–9206, 2019.
- [36] Zhuotao Tian, Hengshuang Zhao, and Michelle Shu *et al.* Prior guided feature enrichment network for few-shot segmentation. *CoRR*, abs/2008.01449, 2020.



- [37] Gen Li, Varun Jampani, and Laura Sevilla-Lara *et al.* Adaptive prototype learning and allocation for few-shot segmentation. In *Proc. IEEE Conf. Comput. Vision Pattern Recognit.*, pages 8334–8343, 2021.
- [38] Bingfeng Zhang, Jimin Xiao, and Terry Qin. Self-guided and cross-guided learning for few-shot segmentation. In *Proc. IEEE Conf. Comput. Vision Pattern Recognit.*, pages 8312–8321, 2021.
- [39] Oriol Vinyals, Charles Blundell, and Tim Lillicrap *et al.* Matching networks for one shot learning. In *Proc. Adv. Neural Inf. Process. Syst.*, pages 3630–3638, 2016.
- [40] Geoffrey E. Hinton, Oriol Vinyals, and Jeffrey Dean. Distilling the knowledge in a neural network. *CoRR*, abs/1503.02531, 2015.
- [41] Sergey Zagoruyko and Nikos Komodakis. Paying more attention to attention: Improving the performance of convolutional neural networks via attention transfer. In *Proc. Int. Conf. Learn. Representations*. OpenReview.net, 2017.
- [42] Tong He, Chunhua Shen, and Zhi Tian *et al.* Knowledge adaptation for efficient semantic segmentation. In *Proc. IEEE Conf. Comput. Vision Pattern Recognit.*, pages 578–587. Computer Vision Foundation / IEEE, 2019.
- [43] Takashi Fukuda, Masayuki Suzuki, and Gakuto Kurata *et al.* Efficient knowledge distillation from an ensemble of teachers. In *Annual Conference of the International Speech Communication Association*, pages 3697–3701. ISCA, 2017.
- [44] Shuchang Lyu, Ting-Bing Xu, and Guangliang Cheng. Embedded knowledge distillation in depth-level dynamic neural network. *CoRR*, abs/2103.00793, 2021.
- [45] Jie Hu, Li Shen, and Gang Sun. Squeeze-and-excitation networks. In *Proc. IEEE Conf. Comput. Vision Pattern Recognit.*, pages 7132–7141. IEEE Computer Society, 2018.
- [46] Sanghyun Woo, Jongchan Park, and Joon-Young Lee *et al.* CBAM: convolutional block attention module. In *Proc. Eur. Conf. Comput. Vision.*, volume 11211 of *Lecture Notes in Computer Science*, pages 3–19. Springer, 2018.
- [47] Kyungyul Kim, Byeongmoon Ji, and Doyoung Yoon *et al.* Self-knowledge distillation: A simple way for better generalization. *CoRR*, abs/2006.12000, 2020.
- [48] Linfeng Zhang, Jiebo Song, and Anni Gao *et al.* Be your own teacher: Improve the performance of convolutional neural networks via self distillation. In *Proc. IEEE Int. Conf. Comput. Vision*, pages 3712–3721. IEEE, 2019.
- [49] Jia Deng, Wei Dong, and Richard Socher *et al.* Imagenet: A large-scale hierarchical image database. In *Proc. IEEE Conf. Comput. Vision Pattern Recognit.*, pages 248–255. IEEE Computer Society, 2009.
- [50] Mennatullah Siam, Boris N. Oreshkin, and Martin Jägersand. AMP: adaptive masked proxies for few-shot segmentation. In *Proc. IEEE Int. Conf. Comput. Vision*, pages 5248–5257. IEEE, 2019.
- [51] Weide Liu, Chi Zhang, and Guosheng Lin *et al.* Crnet: Cross-reference networks for few-shot segmentation. In *Proc. IEEE Conf. Comput. Vision Pattern Recognit.*, pages 4165–4173, 2020.
- [52] Siddhartha Gairola, Mayur Hemani, and Ayush Chopra *et al.* Simpropnet: Improved similarity propagation for few-shot image segmentation. In Christian Bessiere, editor, *IJCAI*, pages 573–579, 2020.
- [53] Yongfei Liu, Xiangyi Zhang, and Songyang Zhang *et al.* Part-aware prototype network for few-shot semantic segmentation. In *Proc. Eur. Conf. Comput. Vision*, pages 142–158. Springer, 2020.
- [54] Mark Everingham, S. M. Ali Eslami, and Luc J. Van Gool *et al.* The pascal visual object classes challenge: A retrospective. *Int. J. Comput. Vision*, 111(1):98–136, 2015.
- [55] Bharath Hariharan, Pablo Andrés Arbeláez, and Ross B. Girshick *et al.* Simultaneous detection and segmentation. In *Proc. Eur. Conf. Comput. Vision.*, volume 8695 of *Lecture Notes in Computer Science*, pages 297–312. Springer, 2014.
- [56] Tao Hu, Pengwan Yang, Chiliang Zhang, and Gang Yu *et al.* Attention-based multi-context guiding for few-shot semantic segmentation. In *AAAI*, pages 8441–8448. AAAI Press, 2019.